

Carbon Nanotubes – PEI – Formate Dehydrogenase Nano-Biointerface for the Specific Bioelectrochemical Reduction of CO₂ to Formate

Mihai-Cristian Fera^a, Rita R. Manuel,^b Inês A. C. Pereira^b, Jose M. Abad^a, Antonio L. De Lacey^a, Marcos Pita^{a*}

^a*Instituto de Catálisis y Petroleoquímica, CSIC, c/Marie Curie 2, 28049 Madrid, Spain*

^b*Instituto de Tecnologia Química e Biológica António Xavier, Universidade Nova de Lisboa, 2780-157 Oeiras, Portugal*

Keywords: W-formate dehydrogenase, carbon nanotubes, bioelectrochemistry, formate, CO₂ reduction

This document is a preprint version of Carbon Volume 209, 5 June 2023, 118013
<https://doi.org/10.1016/j.carbon.2023.118013>

Abstract

Reduction of extensive CO₂ emissions is one of the key challenges that our society must overcome in order to minimize the effects of global warming and climate change. In this respect, electrochemical reduction of CO₂ via redox enzymes is believed to be a promising route to minimize global CO₂ concentrations, as they specifically catalyze the selective CO₂ reduction in a reversible way at low potentials and mild conditions. In this work, we describe the effective anchoring of the enzyme *Desulfovibrio vulgaris* Hildenborough FdhAB formate dehydrogenase using electrostatic interactions favoring oriented immobilization, to the surface of MWCNTs-modified low density graphite electrodes with subsequent protection of the enzyme with polyethyleneimine (PEI) polymer. The synergistic effect of MWCNTs and PEI has been studied. High catalytic current densities, up to -230 μA cm⁻², as well as a high operational stability of 11 h of continuous long-term measurements, were achieved.

Introduction

CO₂ reduction has become a priority research line in order to decrease the impact of greenhouse effect by this gas. Among many possible actions to tackle CO₂ increase, its transformation through chemical reactions is a promising strategy [1]. Therefore, catalysts for performing CO₂ reduction are gaining major research interest. Knowledge on catalysis related to CO₂ reduction is advancing to overcome the state-of-the-art major limitations: the high energy input required and the heterogeneity of reaction products [2]. These challenges can be approached when using biocatalysts such as formate dehydrogenase (FDH), an enzyme that works at physiological conditions and only yields one single product when reducing CO₂ [3]. Although FDHs can have many roles in different organisms, they are often involved in degradation of carbon sources to CO₂ and transfer the electrons to a cofactor, mainly the reduction of NAD⁺ to NADH. There are several examples in which FDH enzymes are able to perform the reverse reaction, taking CO₂ and a cofactor, NADH in most cases, to produce formate and NAD⁺ [4]. However, the activities are very low and require very high concentrations of NADH due to the unfavorable thermodynamics. In contrast, there are some metal-containing FDHs that are independent of NAD⁺/NADH and show high activity for the reduction of CO₂ to HCOO⁻, such as the W-containing FDH, which can be obtained from different organisms such as the bacteria *Desulfovibrio vulgaris* Hildenborough [5], *Bacillus subtilis* [6] or *Clostridium ljundahlii* [7]. This enzyme replaces the typical non-metallic active site with a tungsten cofactor and a set of iron-sulfur clusters to transfer the electrons to/from the redox partner to the active site [5]. *D. vulgaris* W-FDH has been a matter of

research combined with electrochemical means for CO₂ reducing purposes during the latest years, and it is a promising biocatalyst for this purpose. W-FDH can be wired to electrodes both in mediated electron transfer regime and O₂-protected by a redox polymer [8]. It also can work on direct electron transfer regime when adequately interfaced with gold [9], graphite [9] [10] or metal oxide electrodes [11], or with nanomaterials [12]. In a previous work, we observed that the operational stability of W-FDH when covalently bound to low density graphite (LDG) electrodes by carbodiimide coupling was much lower than that measured for hydrogenases or multicopper oxidases covalently immobilized carbon electrodes [13] [14]. This was attributed to the higher vulnerability of W-FDH activity towards covalent modification. In this work, we study an alternative immobilization strategy of W-FDH on LDG electrodes modified with multiwalled carbon-nanotubes' (MWCNTs) adding an electrostatic stabilization stage with polyethyleneimine polymer. These improvements aim at a better performance of the biocathode for reducing CO₂ to formate in aqueous solution.

Materials and Methods

Reagents

All used chemical reagents were purchased from commercial suppliers and employed without any further purification. 4-Nitrobenzene diazonium salt, tetrabutylammonium tetrafluoroborate 99%, DL-dithiothreitol (DTT), polyethyleneimine branched (PEI) 50% w/v, sodium hydrogen carbonate, potassium chloride ultrapure, ethanol absolute grade, multi-walled carbon nanotubes ($\geq 7.5\%$ MWCNTs), 2-(N-morpholino)ethanesulfonic acid (MES 99.5%), 3-(N-morpholino)propanesulfonic acid sodium salt $\geq 99.5\%$, tris(hydroxymethyl)aminomethane (Tris-HCl), acetonitrile and low-density graphite (LDG) (99.9% 3 mm diameter), sodium nitrite, 6-mercapto-1-hexanol, H₂AuCl₄, tetrakis(hydroxymethyl)phosphonium chloride were obtained from Sigma-Aldrich (Merck). Sodium nitrate was obtained from Panreac. Glycerol 10% and HPLC grade *N,N*-dimethyl formamide (DMF) were purchased from Scharlau. Amicon Ultra-0.5 Centrifugal Filter Units Ultracel-50 regenerated cellulose (RC) membrane, 0.5 mL sample volume were obtained from Merck.

All solutions were prepared with Milli-Q grade water (18.2 M Ω ·cm, Millipore) and purged with 99.99% N₂ (Air Liquide) before any further use.

Enzyme preparation

The recombinant W-dependent FdhAB formate dehydrogenase from *D. vulgaris* Hildenborough (DvH-FDH) was isolated and purified as described earlier by *Oliveira et al* [5]. The purified FDH was stored as follows: 100 μ M stock solutions containing 20 mM Tris-HCl, 10% glycerol, and 10 mM NaNO₃ at pH 7.6 were placed at -80 °C. Prior to the enzyme use, the buffer was exchanged to 10 mM MES pH 6.0 by ultrafiltration with 50 kDa cut-off centrifuge filters, and the enzyme was stored in 6 μ L aliquots containing DvH-FDH 27 μ M at -80 °C.

Electrode preparation

LDG rods of 0.3 cm diameter were used as working electrodes. For its use, one edge of each rod was polished for 60 s with emery sandpaper (Buehler), rinsed with MilliQ water, and afterwards sonicated for 10 min in MilliQ water. Finally, the clean electrodes were left to dry at air for 12 h. Before use, the rods' sides were covered with Teflon tape so that the geometric area of the LDG exposed to the solution was 0.07 cm².

Electrode Modification

The surface modification of the electrodes with MWCNTs was carried out as follows: 10 μL of a 1 mg/mL MWCNTs solution in DMF were placed on top of the polished edge of the LDG rod and left to dry at air for 12 h, thus achieving a surface concentration of 0.143 mg/cm².

After the MWCNTs modification, the electrochemical modification with 4-aminophenyl groups was carried out as previously described [13]. Briefly, the modified side of the LDG rod was immersed in a solution consisting of 2 mg of 4-nitrobenzene diazonium salt dissolved in 5 mL of 0.1 M Bu₄NBF₄ prepared in anhydrous CH₃CN, and the potential was cycled twice between 0.6 and -0.6 V (vs. Ag/AgCl) at 200 mV/s. The electrode was then rinsed with MilliQ water and transferred to a 1:9 EtOH:H₂O solution (containing 0.1 M KCl) and the potential was cycled twice between 0 and -1.4 V (vs. Ag/AgCl) at 100 mV/s. Finally, the electrode was rinsed with MilliQ water. A control experiment was performed exactly the same but starting with 20 mg of 4-nitrobenzene diazonium salt.

Afterwards, 20 μL of 16.2 μM DvH-FDH solution in 10 mM MES pH 6.0 buffer were placed by drop-casting, on top of the modified electrodes surface and incubated for 30 min in a humid chamber to allow enzyme rearrangement to yield an oriented binding through dipole moment-driven electrostatic interactions [9]. Following, the modified electrodes were rinsed by immersing them several times in 10 mM MES solution at pH 6.0, and then the immobilized enzyme was activated inside the glovebox by depositing on top of the electrode 20 μL of a 10 mM MES pH 6.0 buffer solution containing 50 mM DTT for 5 min. Finally, 20 μL of a 0.1% w/v polyethyleneimine solution in 10 mM MES pH 6.0 buffer solution was deposited for 30 min on top of the electrode, rinsing afterwards with 10 mM MES pH 6.0 buffer.

Gold-nanoparticle modified LDG electrodes

LDG clean electrodes were modified with gold nanoparticles (average diameter 5 ± 3 nm) following a known procedure [15]. Briefly, the procedure includes a first stage of LDG functionalization with 4-nitrobenzene diazonium salt, the electrochemical reduction of the nitroaryl groups to aminoaryl groups, the covalent immobilization of the gold nanoparticles, and the final functionalization of the gold-carbon surface with an aminoaryl and 6-mercapto-1-hexanol mixed monolayer. The resulting electrodes were modified with FDH and covered with PEI in the same way as the LDG-MWCNT electrodes.

Electrochemical measurements

All electrochemical experiments involving the FDH were carried with an Autolab PGTAT302 potentiostat controlled by NOVA 2.0 software (Metrohm Autolab, The Netherlands) inside a MBraun glovebox with an oxygen content lower than 0.1 ppm. Cyclic voltammetry and chronoamperometry were conducted in a three-electrode glass cell, in which the enzyme-modified LDG rods were used as working electrodes, while a Pt wire (Goodfellow) and a saturated calomel electrode (SCE) (Radiometer Analytical) were used as counter and reference electrodes, respectively. Chronoamperometric measurements were done with magnetic stirring of the electrolyte solution, setting the stirrer at 80 rpm. Impedance Spectroscopy experiments were performed in the same cell configuration using 10 mM ferro-/ferri-cyanide in 10 mM MES buffer, pH 6.0 as electrolyte. Data were collected within the range of frequencies from 10,000 to 1 Hz at a constant bias potential of 0.18 V (vs SCE).

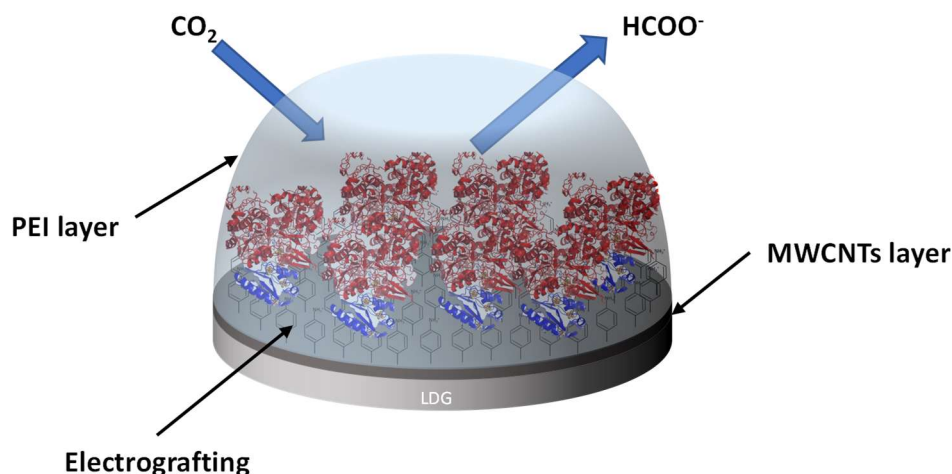
FTIR spectroscopy

FTIR experiments were performed with a Tensor 27 Bruker FTIR instrument with a Whatman gas purge generator. Samples were prepared by depositing on a clean CaF₂ window an aqueous solution of the sample, either PEI 0.1% w/V, PEI + NaHCO₃ 0.55 M, or just 0.55 M NaHCO₃. The samples containing PEI were let to incubate for 30 min and afterwards it was washed with

acetonitrile. The NaHCO_3 sample was left to dry. Afterwards, the modified windows were set into the equipment, allowing the purge to remove the CO_2 from the air in the chamber.

Results and discussion

In order to evaluate the advantage of using nanostructured electrodes as support of FDH immobilization, we modified the LDG electrodes with MWCNTs by means of a drop-cast method. Following, they were functionalized with a layer of aminophenyl (AP) functional groups by an electrografting diazotation method [16]. Such method leads to the electrode functionalization with amino groups for the subsequent oriented controlled immobilization of *DvH*-FDH through electrostatic interactions, facilitating the electrocatalytic activity for CO_2 reduction in DET regime [9]. Finally, the *DvH*-FDH functionalized electrode is covered with PEI, aiming to (i) attract the dissolved substrate to the electrode vicinity and (ii) prevent enzyme desorption and denaturalization. The research strategy followed is schematically described in **Scheme 1**.



Scheme 1. Schematic representation of the LDG/MWCNTs/FDH/PEI electrode for CO_2 reduction. The image includes the crystallographic structure of *DvH*-FDH [5].

The nanostructured electrodes were characterized by several techniques. First of all, we evaluated the effectiveness of the electrode modification with MWCNTs by SEM analysis of both LDG and LDG-MWCNTs electrodes before their functionalization with aminophenyl groups. As expected for a typical bare polished LDG electrode (**Figure 1A**), a slightly porous surface was observed with large portions of smooth area. On the contrary, for the LDG-MWCNTs electrode (**Figure 1B**) a much rougher surface was observed with the characteristic MWCNTs bundles and creeks. The coverage of the electrode by the MWCNTs was also ascertained by cyclic voltammetry employing $\text{Fe}(\text{CN})_6^{3-/4-}$ as electrochemical probes (**Figure 1C**). Reversible faradaic responses for the ferricyanide anion were observed for both LDG and LDG-MWCNT electrodes. However, the latter electrode gave a higher current intensity due to an increase in electrode active area. The current values obtained for LDG cathodic and anodic peaks were $-320 \mu\text{A}$ and $+360 \mu\text{A}$ respectively while for the LDG-MWCNT were $-410 \mu\text{A}$ and $+490 \mu\text{A}$, respectively.

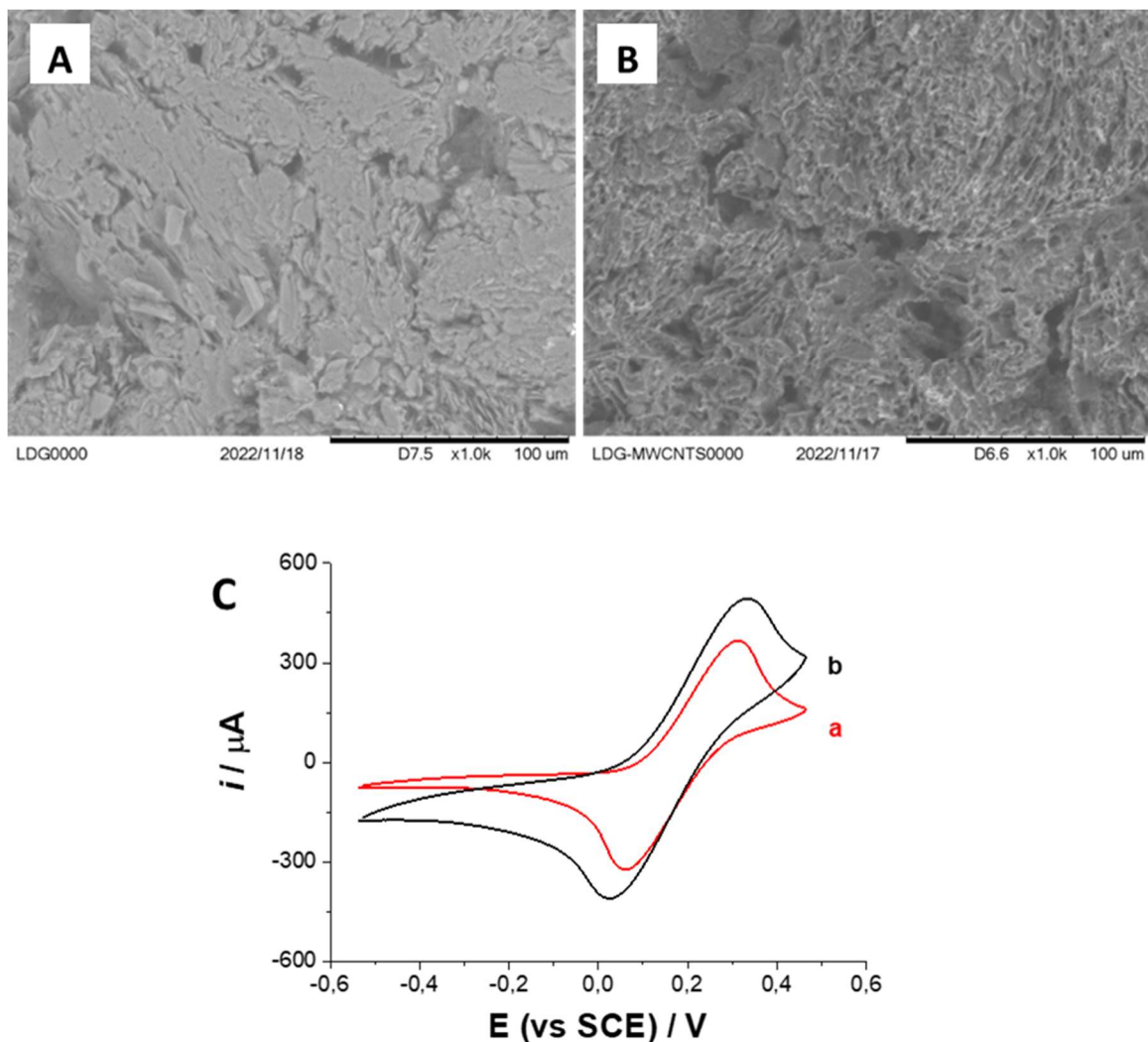


Figure 1: SEM images of (A) a bare LDG electrode and (B) a MWCNTs-modified LDG electrode, with x1000 magnification. (C) Cyclic voltammetry of (a) bare LDG electrode and (b) LDG/MWCNTs electrode. Electrolyte: 10 mM ferro-/ferri-cyanide in 10 mM MES buffer, pH 6.0. Scan rate: 10 mV s⁻¹.

Further, the characterization of the different surface modification steps was carried out by means of electrochemical impedance spectroscopy (**Figure 2A**). The experiments were performed for each modification step in presence of a negatively charged redox probe, Fe(CN)₆^{3-/4-}, which favors electron transfer with positively charged surfaces but hinders it against negatively charged surfaces. The first measurement corresponds to a clean unmodified LDG electrode, which gave a resistance to electron transfer (R_{et}) of 24 Ω , (**Figure 2A line a**). This is a typical value for conductive surfaces like graphite immersed in an electrolyte. After the modification with MWCNTs the electrode was tested again and the R_{et} of the LDG-MWCNTs electrode was 10 Ω , (**Figure 2A line b**), a decrease of 2.5-fold when compared to the bare electrode, demonstrating the conductivity enhancement provided by the MWCNTs. Surface diazotation was assayed by employing two concentrations of diazonium salt: 2 mM and 20 mM, respectively. The 2 mM concentration resulted in an increase of the R_{et} up to 26 Ω for the nitroaryl-modified LDG-MWCNTs electrode, due to the incorporation of nitrophenyl (NP) functional groups. The subsequent reduction of these groups to positively charged aminophenyl (AP) functional groups caused R_{et} to drop to a value of 9 Ω , (**Figure 2A lines c and d**) respectively. By contrast, a significant increase in the resistance was observed when the concentration of the diazonium salt solution was increased ten times, where a R_{et} up to 330 Ω (**Figure S1**) was obtained, which indicated the modification of the electrode surface with an insulation monolayer as previously

reported [17]. This result can be attributed to the formation of nitroaryl multilayers instead of a monolayer, thus increasing the distance between the active site of the enzyme and the electrode surface, which negatively affects the DET regime (*vide infra*). Therefore, maintaining the optimal concentration of 2 mM of diazonium salt determined for non-nanostructured LDG [9] [13] was chosen for further experiments. It should be noted that in that case the amount of functional groups modifying the MWCNTs' surface is in excess being enough for the subsequent immobilization of enzyme units used in the study. This immobilization on the LDG-MWCNTs electrode yielded a slight increase in the R_{et} that can be attributed to the presence of the enzyme and the insulating nature of peptide chains. The addition of PEI caused the decrease of the R_{et} compared to those steps in which the electrode lacked amino-terminated functional groups.

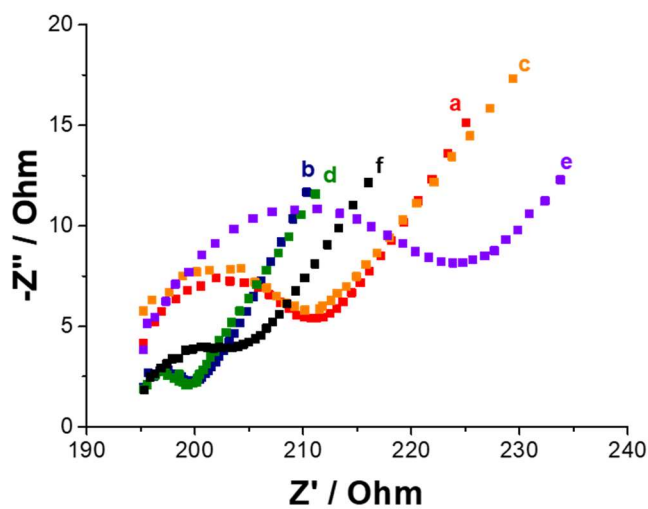


Figure 2. (A) EIS measurements of a bare LDG electrode (red, a), LDG-MWCNTs electrode (blue, b), LDG-MWCNTs-NP electrodes (orange, c) LDG-MWCNTs-AP electrode (green, d), LDG-MWCNTs-AP-FDH electrode (purple, e) and LDG-MWCNTs-AP-FDH-PEI electrode (black, f). Electrolyte: 10 mM ferro-/ferri-cyanide in 10 mM MES buffer, pH 6.0. Frequencies: 10,000 – 1 Hz at a constant applied potential of 0.18 V (SCE).

The modified electrodes containing the *DvH*-FDH enzyme (LDG-MWCNTs-FDH-PEI) were characterized using cyclic voltammetry at pH 6.4 in MOPS_{opt} solution in the presence and absence of dissolved 50 mM NaHCO₃ (**Figure 3A**). The cyclic voltammograms (CVs) in the presence of substrate show the electrochemically enzymatic conversion between CO₂ and formate, which was generated at the electrode surface at lower potentials. A clear catalytic cathodic current is measured in absence of the redox mediator, indicating DET between the enzyme and the electrode. The peaked-shaped oxidation is attributed to the depletion of formate in the electrode surface surrounding due to its uptake by the FDH activity at the less negative potentials. By contrast, the control measurements of the LDG-MWCNTs-FDH-PEI electrode in the absence of substrate gave much lower electrocatalytic CO₂ reduction and formate oxidation currents, which can be attributed to the traces of dissolved CO₂ in the electrolyte. Moreover, control experiments with a LDG-MWCNTs-PEI electrode lacking *DvH*-FDH were carried out, and neither the presence nor absence of substrate yielded any electrocatalytic response (**Figure 3A** lines **c** and **d**). The currents under turnover conditions of CO₂ reduction measured with a LDG-MWCNTs-FDH-PEI electrode reached up to -235 $\mu\text{A cm}^{-2}$ at an applied potential of -0.9 V vs SCE (**Figure 3B b**), considering the geometric area of 0.07 cm² of the LDG electrodes. The chronoamperometry obtained with a LDG-MWCNTs-PEI electrode under the same measurement conditions did not yield any significant change in the signal upon addition of the substrate,

confirming the absence of any faradaic reduction of CO₂ unless W-FDH is properly immobilized on the electrode surface. Thus, confirming that the conversion was catalyzed by the enzyme.

The difference between cathodic currents recorded with the LDG-MWCNTs-FDH-PEI and the LDG-MWCNTs-PEI electrodes at an applied potential of -0.9 V (vs SCE) was calculated to specifically determine the catalytic current density for CO₂ reduction, obtaining a value of -197 $\mu\text{A cm}^{-2}$.

In the case of electrodes functionalized with 20 mM of diazonium salt, a reduction of DET of enzyme and thus electroenzymatic conversion of CO₂ were observed due to the insulated layer as previously described. The enzyme, although immobilized, was not able to transfer electrons directly to the electrode. This was confirmed by the addition of the redox mediator methyl viologen to the solution where mediated electron transfer (MET) led to an increase of 1.5-fold when compared to the DET (**Figure S3 c**). In addition, currents under turnover conditions of CO₂ reduction gave rise to a decrease in both initial current densities and operational stability (**Figure S2**).

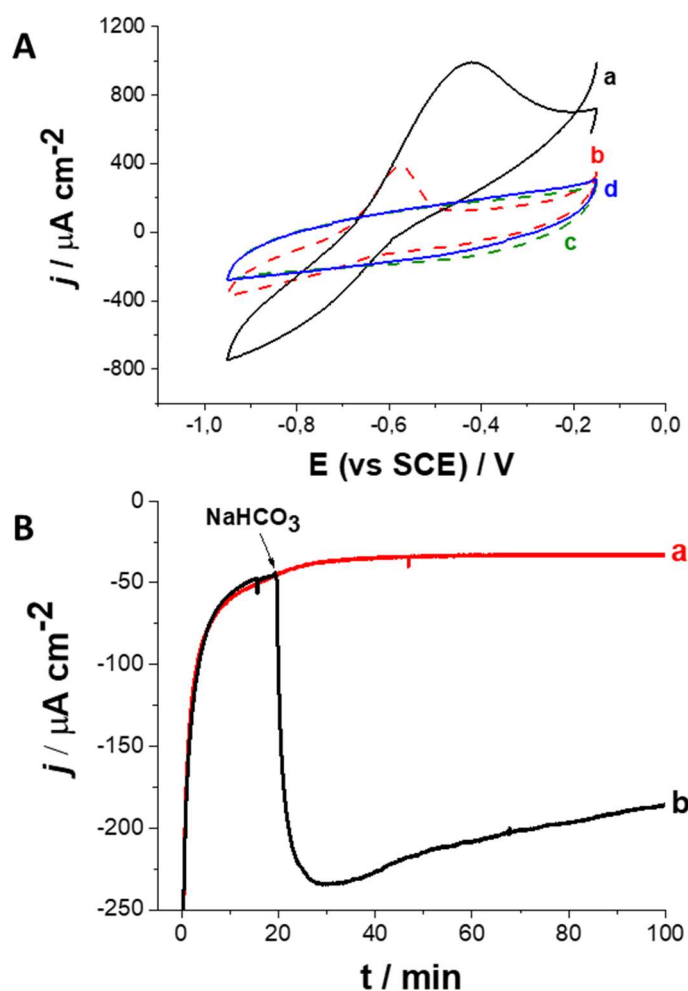


Figure 3. (A) Electrochemical characterization using cyclic voltammetry in the presence (solid lines) and absence (dashed lines) of 50 mM NaHCO₃ of LDG-MWCNTs-FDH-PEI electrode (a-b) and LDG-MWCNTs-PEI electrode (c-d). (B) Chronoamperometry of LDG-MWCNTs-PEI (a) and LDG-MWCNTs-FDH-PEI (b) electrodes. The arrow indicates the moment of 50 mM NaHCO₃ addition to the electrolyte. Electrolyte: MOPS_{opt} (86 mM MOPS and 175 mM KCl), pH 6.4. Scan rate in (A): 10 mV s⁻¹. Applied

potential in (C): -0.9 V vs (SCE). Current densities were calculated with the respect to geometric surface area ($d = 3$ m).

The addition of MWCNTs and PEI to the electrode surface, either separately or combined, affected the initial electrocatalytic activity and the operational stability. We analyzed the remaining catalytic current density after chronoamperometric measurements (**Figure 4A**). First, the LDG-FDH-PEI electrode was compared to an LDG-FDH one, showing that the modification only with PEI caused a moderate increase in both the initial catalytic activity (the most negative current reached just after bicarbonate addition to the electrolyte) and the operational stability (retained current value at the end of the measurement). The improvement of the initial catalytic activity is attributed to the large PEI's affinity towards CO₂ adsorption [18], yielding a greater availability of the enzyme's substrate in the vicinity of the electrode surface. The improvement of the operational stability may be due to the protection of the enzyme that provides its encapsulation within this polymer, as has been reported for other immobilized enzymes [19]. An additional analysis was performed to evaluate the presence of MWCNTs by comparing LDG-FDH, LDG-MWCNTs-FDH, and LDG-MWCNTs-FDH-PEI electrodes. The mere inclusion of the MWCNTs (0.143 mg/cm²) yielded a lower initial bioelectrocatalytic activity but maintained more of the current density over time (**Figure 4A c**), meaning a compromise between lesser maximum catalytic activity and an improvement of the operational stability. On the other hand, the combination of both MWCNTs and PEI modifications caused that both the initial catalytic activity and operational stability benefited from a synergetic effect (**Figure 4A line d, Table 1**).

Another optimization was carried out by studying the amount of MWCNTs deposited on the electrode surface and its consequences on the initial catalytic activity and operational stability of the modified electrodes, **Figure 4B**. On the one hand, the initial catalytic current density increased with increasing MWCNTs concentration deposited on the LDG electrode surface up to a value of 0.214 mg cm⁻², while larger concentrations yielded a pronounced response decrease. On the other hand, it can clearly be observed that the optimal value of MWCNTs superficial concentration for operational stability was 0.143 mg cm⁻². As the goal pursued by adding the MWCNTs is the improvement of the CO₂-reduction biocathode performance in long-duration processes, we determined 0.143 mg cm⁻² as the optimal value of MWCNTs coverage on the electrode.

Table 1. Initial current density upon 50 mM NaHCO₃ addition and retained values after 80 min at -0.9 V vs SCE extracted from **Figure 4A**.

Electrode	Initial current density ($\mu\text{A cm}^{-2}$)	80 min stability (%)
LDG-FDH	-152	57
LDG-FDH-PEI	-171	59
LDG-MWCNTs-FDH	-133	75
LDG-MWCNTs-FDH-PEI	-235	74

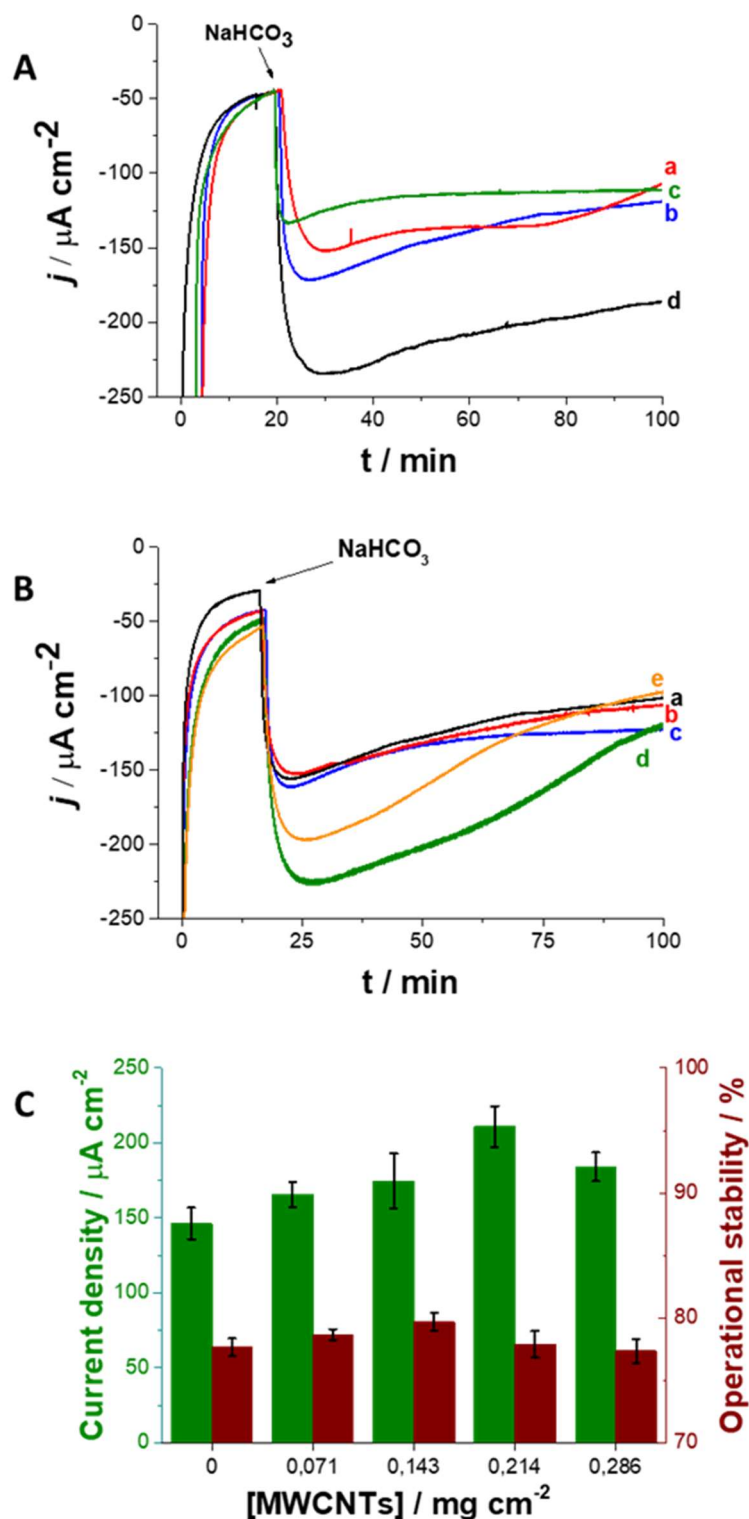


Figure 4. (A) Chronoamperometric measurements at -0.9 V vs SCE of (a) LDG-FDH, (b) LDG-FDH-PEI, (c) LDG-MWCNTs-PEI and (d) LDG-MWCNTs-FDH-PEI electrodes. The arrow indicates the moment of 50 mM NaHCO₃ addition to the electrolyte (86 mM MOPS and 175 mM KCl). (B) Chronoamperometric measurements under the same conditions for LDG-MWCNTs-FDH-PEI electrodes with different amounts of MWCNTs (a) 0 mg cm⁻² MWCNTs/, (b) 0.071 mg cm⁻² MWCNTs/, (c) 0.143 mg cm⁻² MWCNTs/, (d) 0.214 mg cm⁻² MWCNTs/, (e) 0.286 mg cm⁻² MWCNTs/. (C) Initial catalytic currents densities (green, left) and operational stability after 80 min (brown, right) measured for electrodes in (B). Error bars correspond to 3 replicates.

While the MWCNTs effect can be easily explained due to the higher electroactive area of the electrodes thanks to the nanostructuring effect, PEI can contribute to a better response due to (i) improving the immobilization of the W-FDH on the electrode surface or avoiding its leakage and (ii) PEI may also increase the local concentration of CO₂ by an electrostatic attraction effect [18], thus causing a higher initial catalytic current compared to electrodes lacking PEI. This possibility was studied by FTIR spectroscopy, comparing the signals provided by either PEI, NaHCO₃, which is in equilibrium with CO₂ in the electrochemical cell solution, and their combination on a CaF₂ FTIR window, **Figure S4**. The FTIR spectra show that PEI retains NaHCO₃ after 30 min incubation and further washing, showing the characteristic bands of NaHCO₃ molecules, i.e. C=O stretching (2470 cm⁻¹). This result confirms the NaHCO₃ retaining, which is coherent with the substrate preconcentration hypothesis.

We prepared also a control experiment using gold nanoparticles (AuNPs) as nanomaterial for surface enhancement, modifying the LDG surface with covalently-bound AuNPs covered with a mixed monolayer of 4-aminoaryl groups and 6-mercapto-1-hexanol groups [15]. The electrodes were also used as platform for immobilization of FDH covered with PEI. In this case no electrocatalytic effect was obtained in presence of NaHCO₃, which was attributed to the instability of modified AuNPs at the applied negative potentials, Figure S5. This result indicates that not any kind of nanomaterial is valid, and carbon-based ones are more suitable than other typically used nanomaterials.

The long-term operational stability of the optimized LDG-MWCNTs-FDH-PEI electrode for electrocatalytic CO₂ reduction was studied by chronoamperometry at -0.9 V (vs SCE) (**Figure 5A**). The electrode showed an operational stability of at least 11 h, time at which 37% of the initial current density was still maintained. The decrease in current over time was likely due to loss of active immobilized enzyme, as confirmed by a comparison of cyclic voltammograms recorded before and after the long-term measurement (**Figure 5 B** and **C** respectively). This result represents a remarkable improvement when compared with our previous bioelectrocatalytic system with W-FDH covalently linked to LDG electrodes, but lacking MWCNTs and PEI, which only maintained ~10% of its initial activity after 80 min operation (Supporting information of reference [9]). The integration of the total charge produced during several long-term measurements yields a charge value of 0.21 ± 0.01 Coulombs.

To our best knowledge W-FDH has seldom been used under DET regime with other nanostructured carbon-based nanomaterials. It is the case of amino- and carboxy-functionalized CNTs, which show current densities in a similar range of the ones in this work using 2,000 rpm rotation of the electrode [12]. The same work also studies the use of carbon dots but only for biophotocatalytic reduction of CO₂, which is a completely different approach for CO₂ reduction.

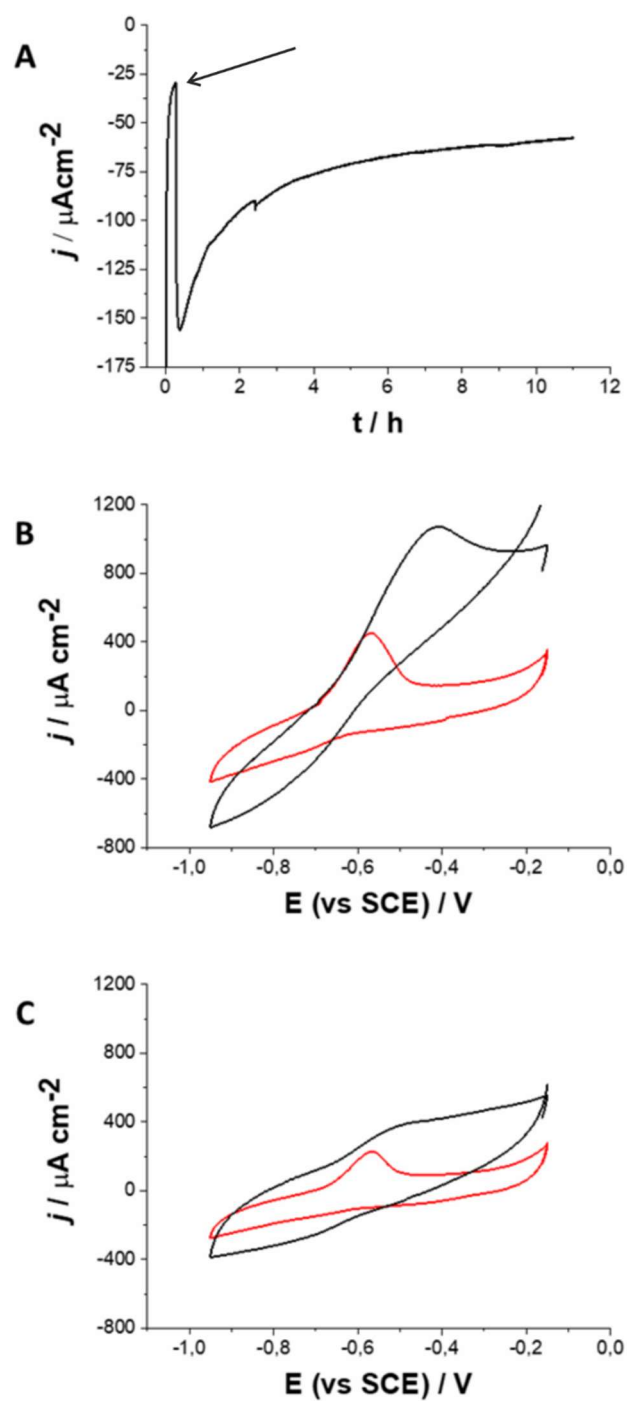


Figure 5. (A) Long-term chronoamperometry with optimized LDG-MWCNTs-FDH-PEI electrode. The arrow indicates the moment of 50 mM NaHCO₃ addition to the electrolyte (86 mM MOPS and 175 mM KCl). Cyclic voltammograms before (B) and after (C) the long-term measurement in the presence (black) and absence (red) of 50 mM NaHCO₃. Electrolyte: MOPS_{opt} (86 mM MOPS and 175 mM KCl), pH 6.39. Applied potential in (A): -0.9 V vs (SCE). Scan rate in (B and C): 10 mV s⁻¹. Current densities were calculated with the respect to geometric surface area ($d = 3$ mm).

Conclusions

We have reported the successful wiring of the recombinant tungsten-dependent FdhAB formate dehydrogenase from *D. vulgaris* Hildenborough (DvH-FDH) on modified LDG electrodes for selective CO₂ reduction under DET regime. The modification of the electrode surface with MWCNTs and the following protection of the electrostatically-wired enzyme with polyethyleneimine showed considerable improvements compared to the same enzyme covalently immobilized directly to LDG [9] in terms of catalytic activity, increasing catalytic current density values up to -235 $\mu\text{A cm}^{-2}$, and operational stability, retaining 37% of the initial catalytic activity after 11 h of continuous long-term measurement. Future work will explore the possibility to extrapolate this synergistic effect to other carbon nanomaterials such as carbon dots, fullerenes or graphene.

Acknowledgments

M. C. Fera acknowledges the Y2020/EMT-6419 “CEOTRES” project funded by the Comunidad Autonoma de Madrid. R. R. Manuel and I. A. C. Pereira acknowledge support from Fundação para a Ciência e a Tecnologia (FCT, Portugal) through fellowship DFA/BD/7897/2020, grant PTDC/BII-BBF/2050/2020, and R&D units MOSTMICRO-ITQB (UIDB/04612/2020 and UIDP/04612/2020) and Associated Laboratory LS4FUTURE (LA/P/0087/2020). A. L. De Lacey acknowledges the PID2021-1241160B-I00 “ELECTROSYSCAT” project funded by MCIN/AEI/ 10.13039/501100011033 and by the European Union. M. Pita and J. M. Abad acknowledge the TED2021-129694B-C22 “DEFY-CO2” project funded by MCIN/AEI/ 10.13039/501100011033 and European Union- NextGenerationEU.

References

- [1] G. Segev, J. Kibsgaard, C. Hahn, Z.J. Xu, W.-H. (Sophia) Cheng, T.G. Deutsch, C. Xiang, J.Z. Zhang, L. Hammarström, D.G. Nocera, A.Z. Weber, P. Agbo, T. Hisatomi, F.E. Osterloh, K. Domen, F.F. Abdi, S. Haussener, D.J. Miller, S. Ardo, P.C. McIntyre, T. Hannappel, S. Hu, H. Atwater, J.M. Gregoire, M.Z. Ertem, I.D. Sharp, K.-S. Choi, J.S. Lee, O. Ishitani, J.W. Ager, R.R. Prabhakar, A.T. Bell, S.W. Boettcher, K. Vincent, K. Takanabe, V. Artero, R. Napier, B.R. Cuenya, M.T.M. Koper, R.V.D. Krol, F. Houle, The 2022 solar fuels roadmap, *J. Phys. D: Appl. Phys.* 55 (2022) 323003. <https://doi.org/10.1088/1361-6463/ac6f97>.
- [2] M.G. Kibria, J.P. Edwards, C.M. Gabardo, C.-T. Dinh, A. Seifitokaldani, D. Sinton, E.H. Sargent, Electrochemical CO₂ Reduction into Chemical Feedstocks: From Mechanistic Electrocatalysis Models to System Design, *Advanced Materials*. 31 (2019) 1807166. <https://doi.org/10.1002/adma.201807166>.
- [3] J.R. Andreesen, E. El Ghazzawi, G. Gottschalk, The effect of ferrous ions, tungstate and selenite on the level of formate dehydrogenase in *Clostridium formicoaceticum* and formate synthesis from CO₂ during pyruvate fermentation, *Arch. Microbiol.* 96 (1974) 103–118. <https://doi.org/10.1007/BF00590167>.
- [4] M. Meneghello, C. Léger, V. Fourmond, Electrochemical Studies of CO₂-Reducing Metalloenzymes, *Chemistry - A European Journal*. 27 (2021) 17542–17553. <https://doi.org/10.1002/chem.202102702>.
- [5] A.R. Oliveira, C. Mota, C. Mourato, R.M. Domingos, M.F.A. Santos, D. Gesto, B. Guigliarelli, T. Santos-Silva, M.J. Romão, I.A. Cardoso Pereira, Toward the Mechanistic Understanding of Enzymatic CO₂ Reduction, *ACS Catal.* 10 (2020) 3844–3856. <https://doi.org/10.1021/acscatal.0c00086>.
- [6] M. Meneghello, A. Uzel, M. Broc, R.R. Manuel, A. Magalon, C. Léger, I.A.C. Pereira, A. Walburger, V. Fourmond, Electrochemical Kinetics Support a Second Coordination

- Sphere Mechanism in Metal-Based Formate Dehydrogenase, *Angew Chem Int Ed.* 62 (2023). <https://doi.org/10.1002/anie.202212224>.
- [7] W. Li, Y. Gao, X. Sun, L. Wan, H. Ji, H. Luo, Y. Tian, H. Song, G. Wu, L. Zhang, Direct detection of a single [4Fe-4S] cluster in a tungsten-containing enzyme: Electrochemical conversion of CO₂ into formate by formate dehydrogenase, *Carbon Energy.* (2023) cey2.304. <https://doi.org/10.1002/cey2.304>.
- [8] J. Szczesny, A. Ruff, A.R. Oliveira, M. Pita, I.A.C. Pereira, A.L. De Lacey, W. Schuhmann, Electroenzymatic CO₂ Fixation Using Redox Polymer/Enzyme-Modified Gas Diffusion Electrodes, *ACS Energy Lett.* 5 (2020) 321–327. <https://doi.org/10.1021/acsenerylett.9b02436>.
- [9] J. Alvarez-Malmagro, A.R. Oliveira, C. Gutiérrez-Sánchez, B. Villajos, I.A.C. Pereira, M. Vélez, M. Pita, A.L. De Lacey, Bioelectrocatalytic Activity of W-Formate Dehydrogenase Covalently Immobilized on Functionalized Gold and Graphite Electrodes, *ACS Appl. Mater. Interfaces.* 13 (2021) 11891–11900. <https://doi.org/10.1021/acsami.0c21932>.
- [10] M. Meneghello, A.R. Oliveira, A. Jacq-Bailly, I.A.C. Pereira, C. Léger, V. Fourmond, Formate Dehydrogenases Reduce CO₂ Rather than HCO₃⁻: An Electrochemical Demonstration, *Angewandte Chemie International Edition.* 60 (2021) 9964–9967. <https://doi.org/10.1002/anie.202101167>.
- [11] M. Miller, W.E. Robinson, A.R. Oliveira, N. Heidary, N. Kornienko, J. Warnan, I.A.C. Pereira, E. Reisner, Interfacing Formate Dehydrogenase with Metal Oxides for the Reversible Electrocatalysis and Solar-Driven Reduction of Carbon Dioxide, *Angewandte Chemie International Edition.* 58 (2019) 4601–4605. <https://doi.org/10.1002/anie.201814419>.
- [12] V.M. Badiani, C. Casadevall, M. Miller, S.J. Cobb, R.R. Manuel, I.A.C. Pereira, E. Reisner, Engineering Electro- and Photocatalytic Carbon Materials for CO₂ Reduction by Formate Dehydrogenase, *J. Am. Chem. Soc.* 144 (2022) 14207–14216. <https://doi.org/10.1021/jacs.2c04529>.
- [13] C. Vaz-Dominguez, S. Campuzano, O. Rüdiger, M. Pita, M. Gorbacheva, S. Shleev, V.M. Fernandez, A.L. De Lacey, Laccase electrode for direct electrocatalytic reduction of O₂ to H₂O with high-operational stability and resistance to chloride inhibition, *Biosensors and Bioelectronics.* 24 (2008) 531–537. <https://doi.org/10.1016/j.bios.2008.05.002>.
- [14] M.A. Alonso-Lomillo, O. Rüdiger, A. Maroto-Valiente, M. Velez, I. Rodríguez-Ramos, F.J. Muñoz, V.M. Fernández, A.L. De Lacey, Hydrogenase-Coated Carbon Nanotubes for Efficient H₂ Oxidation, *Nano Lett.* 7 (2007) 1603–1608. <https://doi.org/10.1021/nl070519u>.
- [15] C. Gutiérrez-Sánchez, M. Pita, C. Vaz-Domínguez, S. Shleev, A.L. De Lacey, Gold Nanoparticles as Electronic Bridges for Laccase-Based Biocathodes, *J. Am. Chem. Soc.* 134 (2012) 17212–17220. <https://doi.org/10.1021/ja307308j>.
- [16] P. Allongue, M. Delamar, B. Desbat, O. Fagebaume, R. Hitmi, J. Pinson, J.-M. Savéant, Covalent Modification of Carbon Surfaces by Aryl Radicals Generated from the Electrochemical Reduction of Diazonium Salts, *J. Am. Chem. Soc.* 119 (1997) 201–207. <https://doi.org/10.1021/ja963354s>.
- [17] P.A. Brooksby, A.J. Downard, Electrochemical and Atomic Force Microscopy Study of Carbon Surface Modification via Diazonium Reduction in Aqueous and Acetonitrile Solutions, *Langmuir.* 20 (2004) 5038–5045. <https://doi.org/10.1021/la049616i>.
- [18] E.P. Dillon, C.A. Crouse, A.R. Barron, Synthesis, Characterization, and Carbon Dioxide Adsorption of Covalently Attached Polyethyleneimine-Functionalized Single-Wall Carbon Nanotubes, *ACS Nano.* 2 (2008) 156–164. <https://doi.org/10.1021/nn7002713>.
- [19] J.J. Virgen-Ortíz, J.C.S. dos Santos, Á. Berenguer-Murcia, O. Barbosa, R.C. Rodrigues, R. Fernandez-Lafuente, Polyethylenimine: a very useful ionic polymer in the design of immobilized enzyme biocatalysts, *J. Mater. Chem. B.* 5 (2017) 7461–7490. <https://doi.org/10.1039/C7TB01639E>.